Chapter 5

Optical diffraction in non-uniform cholesterics-phase grating effect

5.1 Introduction

In the previous chapters, we were concerned with the light scattering due to the dynamics of the director. The director dynamics have short characteristic time scales of the order of a few milliseconds. However, on longer time scales these thermal fluctuations average out resulting in an average helical structure which has its own interesting optical properties. In this chapter we consider some of these properties of cholesterics and effects of static structural non-uniformities in them.

Cholesterics exhibit many interesting optical properties like selective Bragg reflection, anomalous optical rotation and diffraction in the phase grating geometry [1]. These interesting features arise from the fact that the cholesteric has a locally uniaxial structure whose symmetry axis twists uniformly about an orthogonal direction. Most of the cholesterics have a pitch comparable to the wavelength of visible light. The optics of cholesterics is usually studied either in the Bragg geometry or in the phase grating geometry. These two geometries are described in the following sections.

5.1.1 The Bragg geometry

In the Bragg geometry, light of appropriate wavelength and polarization, incident in a direction parallel or at an angle to the twist axis undergoes reflection. It is akin to Bragg reflection of x-rays from crystals but with a subtle difference. For example,

a right handed cholesteric reflects right circularly polarized light and transmits left circularly polarized light. The cigenmodes of propagation in such a structure are circularly polarized states with opposite handedness. It is well known that in a uniform cholesteric of pitch P, the width of the reflectiori band is given by

$$\Delta\lambda = (\mu_e - \mu_o)P \tag{5.1}$$

Where μ_o and μ_e are the ordinary and the extraordinary refractive indices respectively of the local uniaxial structure. This reflection band is centered at a wavelength λ_o given by

$$\lambda_o = \bar{\mu}P \tag{5.2}$$

where $\bar{\mu}$ is the average refractive index of tlie cholesteric.

In the Bragg geometry there have been some studies on non-uniform cholesterics. Mazkedian and Bartolino [2], **[3]** produced a gradient in the pitch by compressing a cholesteric along its twist axis. Their experiments were performed in the Bragg geometry with oblique incidence of light. They observed small changes in λ_o with the applied pressure. Recently, Broer et. al., **[4]** prepared a pitch gradient cholesteric and observed that the non-uniformity results in a very wide reflection band. In their system, the pitch uniformly increases from one end of the sample to the other. These investigators used a sophisticated polymerization diffusion technique to create large gradients in the cholesteric pitch. Usual cliolesterics, typically have a Bragg width AX of the order of 50 nm. In the system studied by Broer et. al., the pitch varied frorn **230** nm at one end of the sample to almost double this value at the other end. They demonstrated that in the process AX considerably increased to a value as high as 350 nm. For their pitch gradient cholesteric the width of the reflection band is given by

$$\Delta\lambda = P_{max}\,\mu_e - P_{min}\,\mu_o$$

Here, P_{max} and P_{min} are respectively the smallest and largest values of the pitch asso-

ciated with the structure. Wide band reflectors made from pitch gradient cholesterics with reflection band in the visible region find many applications.

5.1.2 The phase grating geometry

A phase grating is a structure with periodic spatial refractive index variations. If a plane wavefront of light encounters such a structure, different portions of the wavefront will traverse different optical paths leading to a corrugated wavefront on emergence. Raman and Nath [5] gave a theory to explain the phase gratings generated by density modulations in an isotropic liquid. The density modulations were created by producing a standing ultrasonic wave in the liquid.

For light of appropriate polarization and wavelength, the cholesteric can act as a phase grating. This is shown in figure(5.1). Here, the refractive index modulation occurs due to the birefringence and helical structure of the cholesteric.

In the phase grating geometry, linearly polarized light with electric vector normal to the twist axis is incident in a direction perpendicular to the direction of the twist axis of the cholesteric. Such a beam undergoes diffraction. The diffraction properties have been studied extensively in the case of uniform cholesterics, that is, cholesterics of uniform pitch [1], [6]. Sackmann et. al., [7] were the first to experimentally study a cholesteric in the phase grating geometry. They found that for light polarized in a direction perpendicular to the helix axis, all diffraction orders are also linearly polarized in the same direction as the incident light. The relative intensities of the different orders depend on factors like sample thickness, wavelength of light and effective local refractive index.

In the present chapter, we carry out a systematic study of the effects of non-uniformities in the cholesteric structure on the phase grating properties. The non-uniformity being in the nature of a gradient in the pitch. Cholesteric pitch can become non-uniform either due to surface effects or inherent strains. We first briefly discuss the well known theory of diffraction from uniform cholesterics and then develop our model for

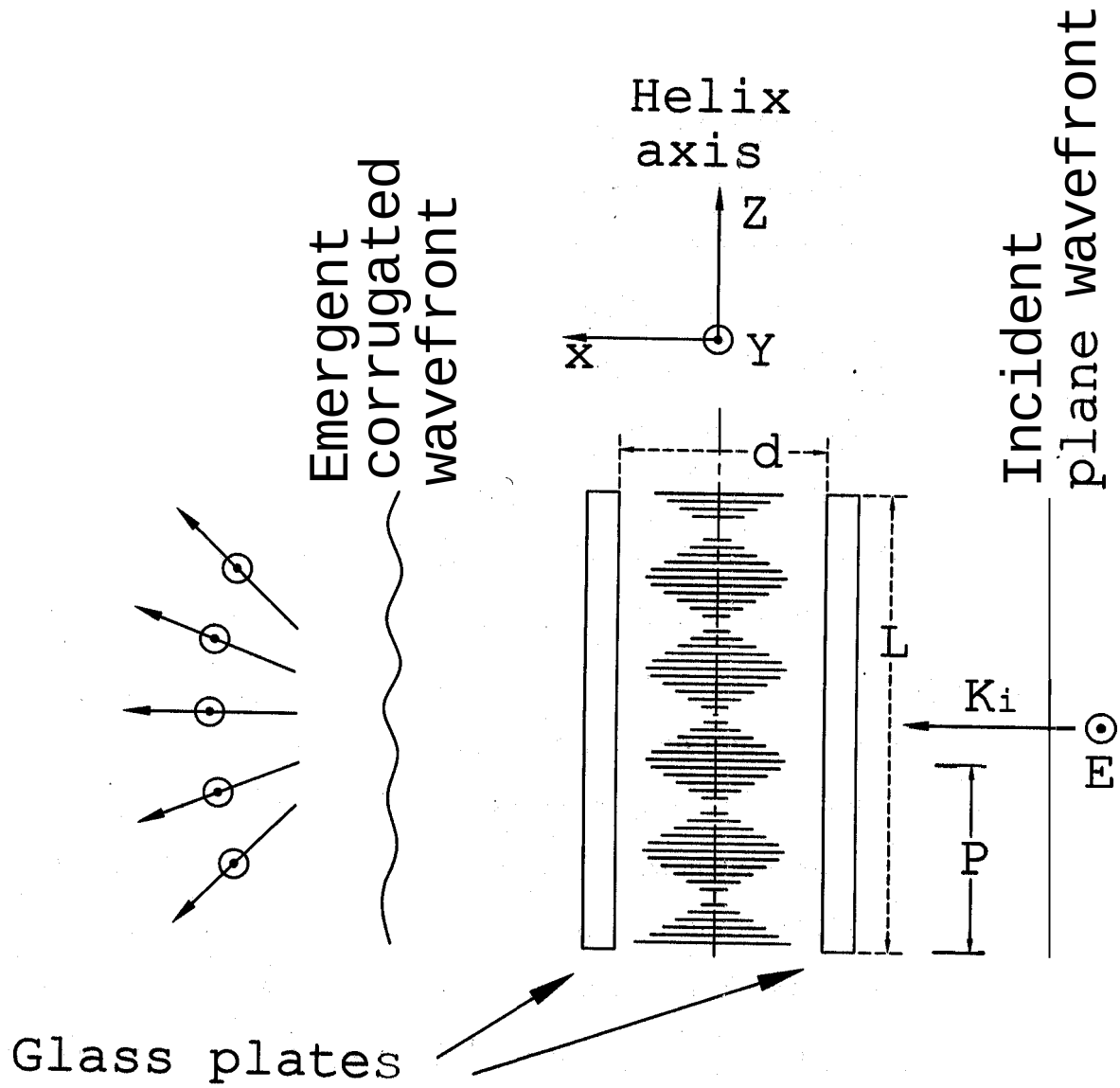

Figure 5.1: Schematic representation of a cholesteric aligned in the phase grating geometry. A plane wavefront incident in a direction $\mathbf{K}_i$ normal to the twist axis of the sample with its electric vector E, perpendicular to the twist axis encounters a varying refractive index and emerges as a corrugated wavefront, resulting in diffraction. L is the lateral sample size and d is the sample thickness.

non-uniform cholesterics.

5.2 Theory of diffraction

In this section we give an outline of the theory used by us to calculate the diffraction pattern from cholesterics in the phase grating geometry. We consider a plane wavefront of linearly polarized light of unit amplitude to be incident in a direction perpendicular to the twist axis of a cholesteric. The direction of polarization is also perpendicular to the twist axis. For such a light beam the refractive index of the medium is a periodic function of position. The plane wavefront emerges as a corrugated wave front. Thus, the cholesteric acts as a one dimensional grating. The Fourier transform of this corrugated wavefront gives the amplitude of the wave diffracted in a particular direction. Here, we make use of the Raman-Nath (RN) approximation. According to the RN approximation, the wavelength of the phase fluctuation in the cholesteric is large compared to its amplitude and the wavelength of the incident light [5],[6]. This assumption allows us to neglect the internal reflections in the medium. The RN approximation is valid only for small values of $\Delta\mu$d. An important assumption of the RN theory was that the emergent wavefront was perfectly sinusoidal. Hence, the entire diffraction pattern could be analytically calculated. This led to the well known result of the intensities of the successive diffraction orders following the Bessels function law. However, in cholesterics the situation is quite different. The emergent wavefront is no longer purely sinusoidal and it is not possible to analytically workout its Fourier transform [6]. The problem becomes even more intractable, in the case of non-uniform cholesterics where the emergent wavefront might not be even periodic. Hence, we seek numerical solutions to this problem using well known Fourier transform computational techniques.

5.2.1 Uniform cholesterics

Let us consider a cholesteric aligned with its twist axis along the z axis and the direction of the incident light along the x axis as shown in figure(5.1).

In a uniform cholesteric, the director rotates uniformly in space and the components of the director are given by,

$$n_x = cos(q_o z)$$

$$n_y = sin(q_o z)$$

$$n_z = 0$$

Where, $q_o = 2\pi/P$. For a uniform cholesteric, the effective local refractive index μ_{l_o} as seen by the incident light polarized in the y direction is given by,

$$\frac{1}{\mu_{l_o}^2} = \frac{n_x^2(z)}{\mu_e^2} + \frac{n_y^2(z)}{\mu_o^2} \tag{5.3}$$

5.2.2 Non-uniform cholesterics

We now consider non-uniform cholesterics where the non-uniformity is in the nature of a gradient in the pitch. We consider only linear variations in the pitch. We focus our attention to two types of non-uniform cholesterics. In one type, the pitch gradient is symmetric with respect to the sample center. We refer to such samples as the type-I cliolesterics. In the other type, the pitch gradient is asymmetric with respect to the sample center. We refer to these as the type-I1 cholesterics. The type-I cholesterics can be further classified into type-Ia and type-1b. In the type-Ia cholesteric the pitch decreases uniformly from the center of the sample as we move towards the end of the sample and in type-Ib cholesteric, the pitch uniformly increases as we move towards the end of the sample. In the type-I1 cholesteric the pitch uniformly increases from one end of the sample to the other end. The refractive index profiles of the type-Ia and the type-I1 cholesterics are shown in figure(5.2).

In a non-uniform cholesteric with a gradient in the pitch, we assume the components of the director to bc:

$$n_x = cos(q'z + \phi')$$

$$n_y = sin(q'z + \phi')$$

$$n_z = 0$$

Where $q' = (q, + \epsilon_g)$ is the local wavevector of the non-uniform cholesteric and ϵ_g is a gradient parameter. For the pitch gradient cholesteric, the local refractive index, μ_l is given by equation(5.3) but with the above n_x and n_y.

In the followingsections we describe the different models of non-uniformity in cholesterics.

Type-I structures

The type-I structures have a refractive index profile of the type illustrated in figure(5.2a). In our calculations we have used the following simple expression for the gradient parameter ϵ_g to obtain the non-uniformity in the type-Ia structure.

$$\epsilon_g = \frac{q_o}{P_{def}} (|z|) \frac{1}{L} \tag{5.4}$$

Here, L is the lateral sample size and P_{def} is a deformation parameter whose value is selected to produce the required non-uniformity in the pitch. The z coordinate runs from $-L/2$ to $L/2$ with a spatial sampling interval of 0.5μm.

The type-Ib structure is generated by,

$$\epsilon_g = \frac{q_o}{P_{def}} \left(\frac{L}{2} - |z|\right) \frac{1}{L} \tag{5.5}$$

Here also the range of z is from $-L/2$ to L/2 with a spatial sampling interval of 0.5μm.

Type-I1 structures

The type-I1 structures are asymmetric about their centers. The pitch uniformly increases from one end of the sample to the other. Its refractive index profile is illustrated in figure (5.2b). A simple form for ϵ_g that generates such a structure is,

$$\epsilon_g = \frac{q_o}{P_{def}} (z) \frac{1}{L} \tag{5.6}$$

Here the range of z is from 0 to L with a spatial sampling interval of 0.5μm.

In the next section we describe features of input beams that we have used in our calculations of the diffraction patterns.

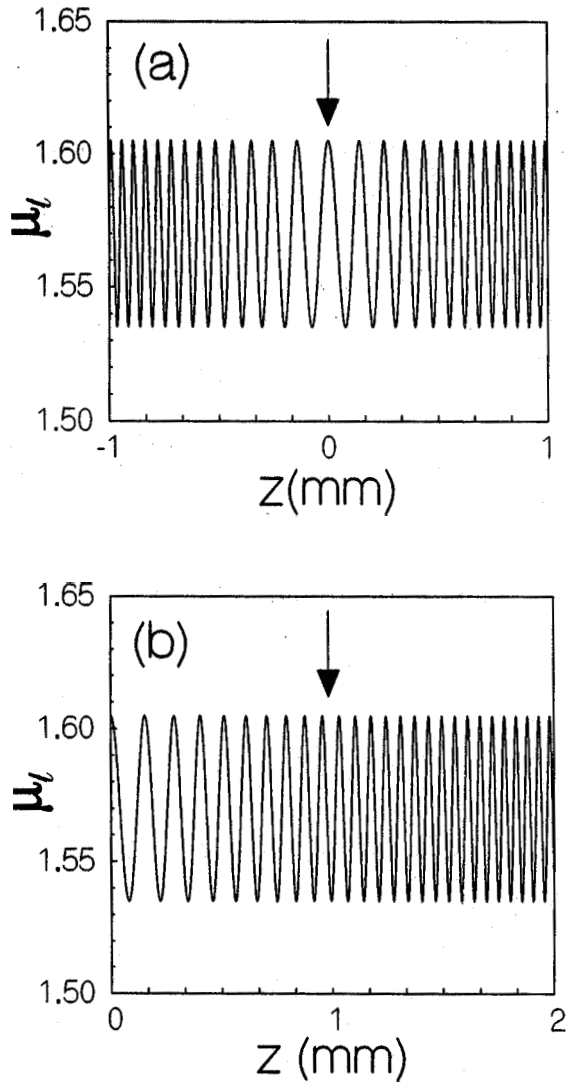

Figure **5.2:** An exaggerated view of the refractive index μ_l as a function of position z. (a) In a type-Ia cholesteric, the refractive index profile is symmetric with respect to the center of the sample. (b) In a type-I1 cholesteric, the refractive index profile is asymmetric with respect to the center of the sample. In both the cases, the center of the sample is indicated by the arrow.

Unifarm and Gaussian input beams

The diffraction pattern obtained from a grating will depend on the intensity distribution of the input beams. We have computed the diffraction patterns arising out of two kinds of parallel input beams; a beam with a uniform intensity or equivalently amplitude profile and a beam with a Gaussian intensity or equivalently Gaussian amplitude profile.

In the case of the uniform beam the emergent wavefront is described by

$$U(z) = e^{2\pi i \mu_l d/\lambda} \tag{5.7}$$

Where λ is the wavelength of light.

For a uniform beam, the amplitude $A_U(k)$ of the diffracted wave in the direction ψ relative to the main beam is given by,

$$A_U(k) = \int_{-L/2}^{+L/2} e^{2\pi i \mu_l d/\lambda}\, e^{-ikz} dz \tag{5.8}$$

Where k $= (2\pi/\lambda) sin(\psi)$.

For a Gaussian beam, the amplitude $A_G(k)$ of the diffracted wave is given by,

$$A_G(k) = \int_{-L/2}^{+L/2} e^{-(z/\sigma)^2}\, e^{2\pi i \mu_l d/\lambda}\, e^{-ikz} dz \tag{5.9}$$

Where a is the Gaussian amplitude width. When L$\rightarrow \infty$ these integrals become standard Fourier transforms.

We have worked out these integrals numerically. The numerical algorithm used to perform the integration is the radix-2 FFT algorithm [8]. In our computations, we used experimentally realizable parameters for the pitch, birefringence, wavelength of light and sample thickness.

5.3 Results

In this section we shall describe the salient features of our computed diffraction patterns from non-uniform cholesterics. The diffraction patterns arising out of uniform

and Gaussian input beams are given in separate subsections. Our results are presented as normalized intensities of different diffraction orders. We have taken an intensity level of 10^{-4} as the lower limit of detection.

We have assumed the following experimentally realizable values for the parameters used in all our calculations:

- Birefringence $\Delta\mu = 0.07$
- Lateral sample size L = 100 pitches
- Sample thickness d = 15μm
- Wavelength of light $\lambda = 0.633\ \mu$m

In order to highlight the effects of non-uniformities, we also give for comparison the diffraction pattern to be expected in the case of uniform cholesterics.

5.3.1 Diffraction of uniform beams

In this section we describe the results obtained for uniform input beams. The input beam is a plane wavefront of infinite extent. In figure(5.3) we show the diffraction pattern from a uniform cholesteric illuminated with a uniform beam. The pitch of the cholesteric is 20μm. One can see six sharp diffraction orders on either side of the zeroth order. The orders have practically no width. We can notice that some of the higher diffraction orders are more intense than lower ones. This is a characteristic feature of phase gratings. In amplitude gratings, intensities of the orders monotonically decrease as we goes to higher orders. In all our calculations diffracted intensity has been normalized relative to that of the incident beam. In figure(5.4) we show the diffraction from a type-Ia sample where the pitch at the center is 5% more than the pitch at the ends . One can see that the orders are broad and have irregular intensity profiles. When the pitch gradient is increased such that pitch at the center is 50% higher than the ends, the higher orders become so broad that they merge into each other. This is clearly indicated by the pattern shown in figure(5.5). We would like to point out that the diffraction pattern for the uniform input beam is very similar for the type-Ia and type-Ib structures. Further,

the diffraction patterns from the type-Ia and type-Ib samples are strictly symmetric about the zeroth order.

Figure(5.6) shows the diffraction pattern from a type-I1 structure where the gradient is such that the pitch at the center is 5% higher than the pitch at the lower end. The orders become broad and have regular features in their intensity 'profiles. Each order is very nearly symmetric about its center. Here again, as we go to higher orders the widths of the orders increase.

For the diffraction pattern shown in figure(5.7) the gradient is such that the pitch at the center is 50% higher than the pitch at the lower end. We notice that the intensities of the orders fall and that they become much broader. Orders higher than ± 1 have merged with one another.

5.3.2 Diffraction of Gaussian beams

We shall now describe the diffraction patterns arising from the type-Ia, type-Ib and type-I1 structures with various degrees of non-uniformities illuminated with Gaussian input beams.

In figure(5.8) we show the diffraction pattern of a uniform cholesteric. In our calculations we have taken the value of the Gaussian amplitude width a to be equal to lmm. Hence the Gaussian intensity width will be equal to $1/\sqrt{2}$mm which is much smaller compared to the lateral size of 2mm. We may notice that the diffraction orders are very sharp without any broadening.

In figure(5.9) we depict the diffraction pattern from a type-Ia cholesteric. The cholesteric has a pitch gradient such that the pitch at the center of the sample is 5% higher than the pitch at the ends. Here the important feature to notice is that each order has an asymmetric saw-tooth like profile. The direction of tapering of the profiles of the orders is away from the zeroth order. In figures(5.10) and (5.11) we show the effects of increasing the gradient to values such that the pitch at the center is 20% and 50% respectively more than that at the sample ends. We notice that with increasing pitch gradient, the profiles of the orders become broader and their asym-

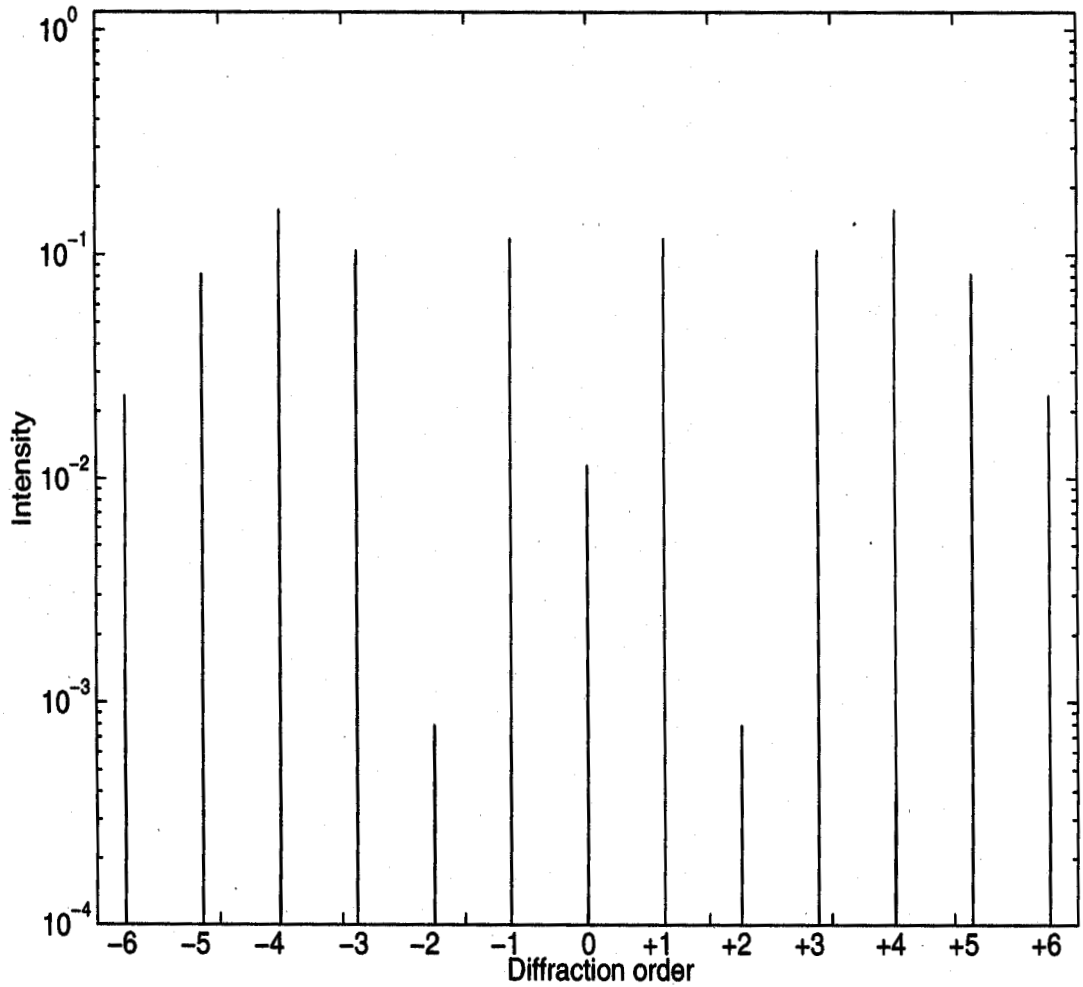

Figure **5.3:** Diffraction pattern of a uniform cholesteric with a uniform input beam. The pitch of the cholesteric is $20\mu m$. The diffraction intensities are normalized with respect to that of the incident beam.

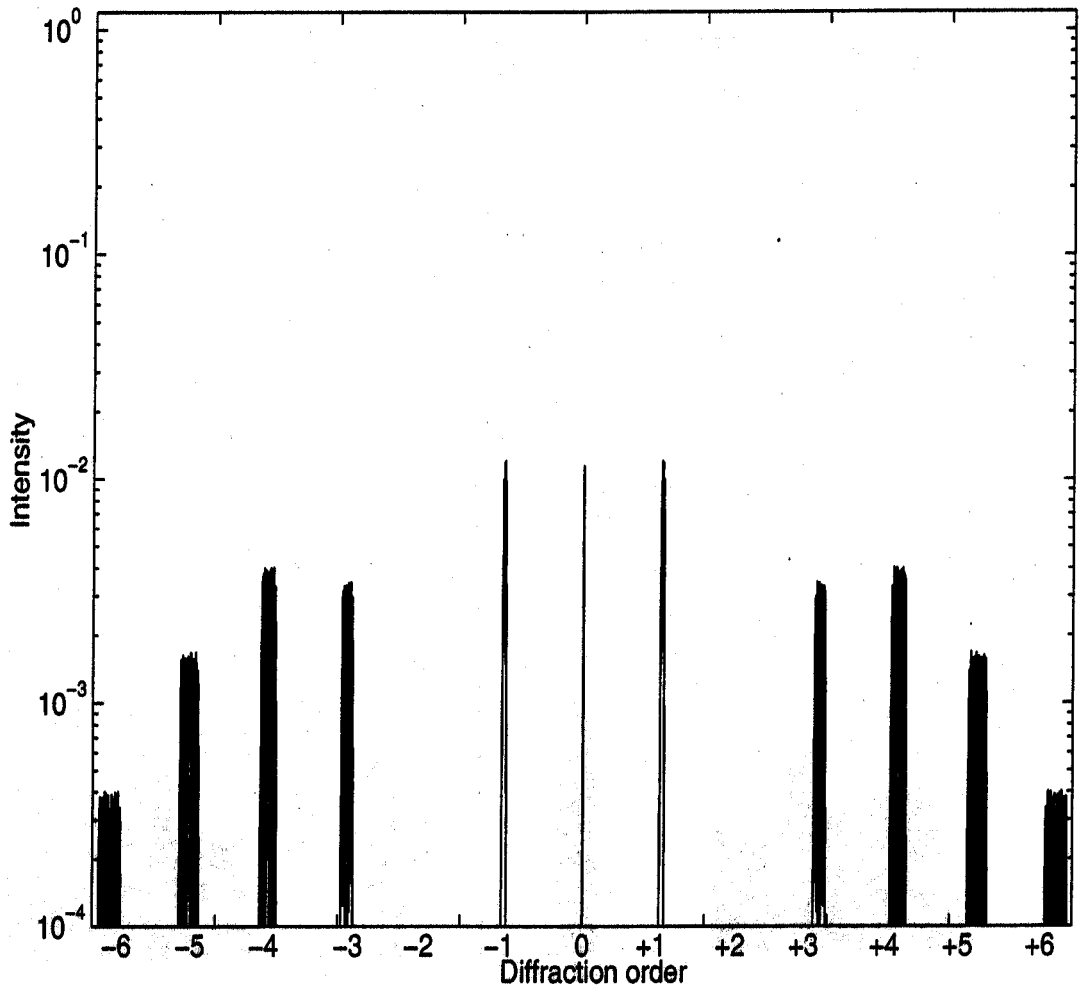

Figure 5.4: Diffraction pattern of a type-la cholesteric structure with a uniform input beam. Here the pitch at the sample center is 21pm and the pitch at the ends is 20μm.

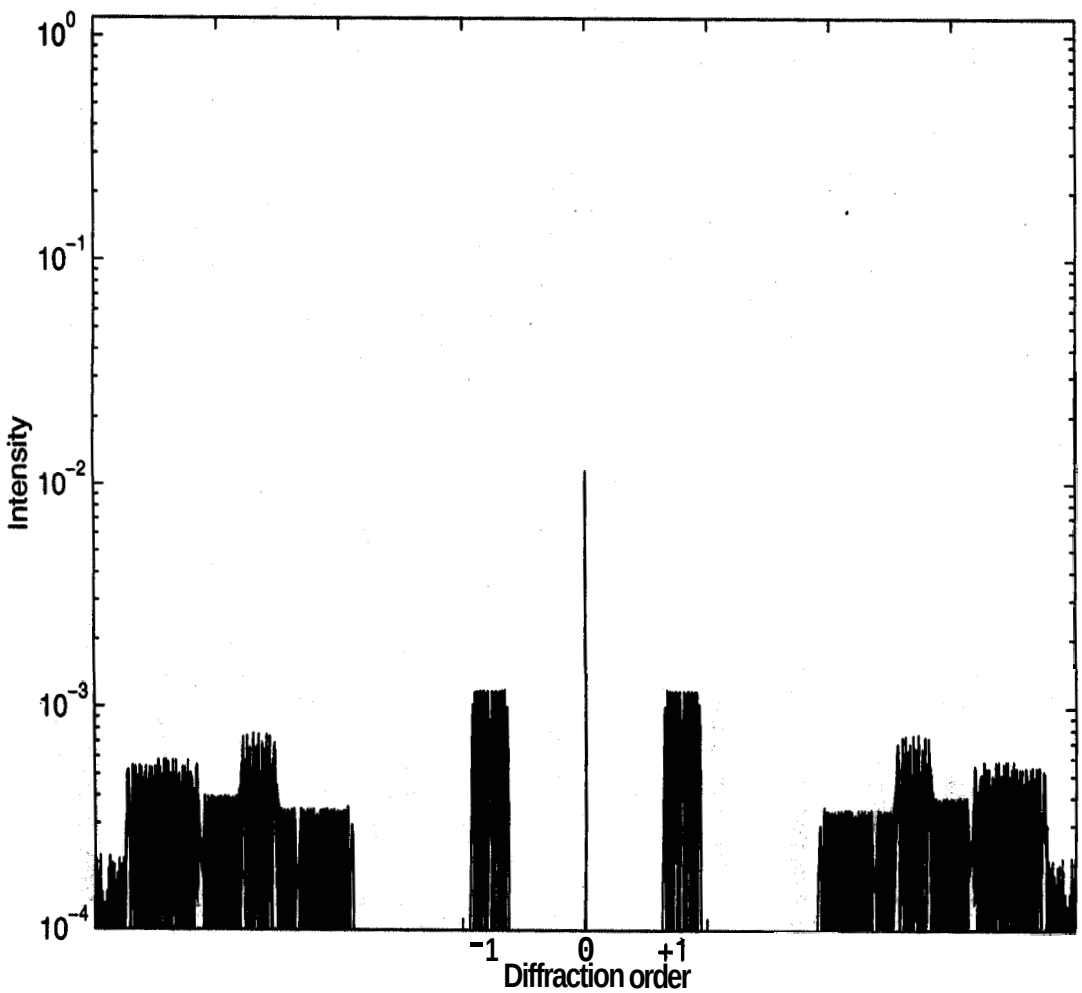

Figure 5.5: Diffraction from a type-Ia sample where the pitch at the sample center is 30μm and at the sample ends is 20μm.

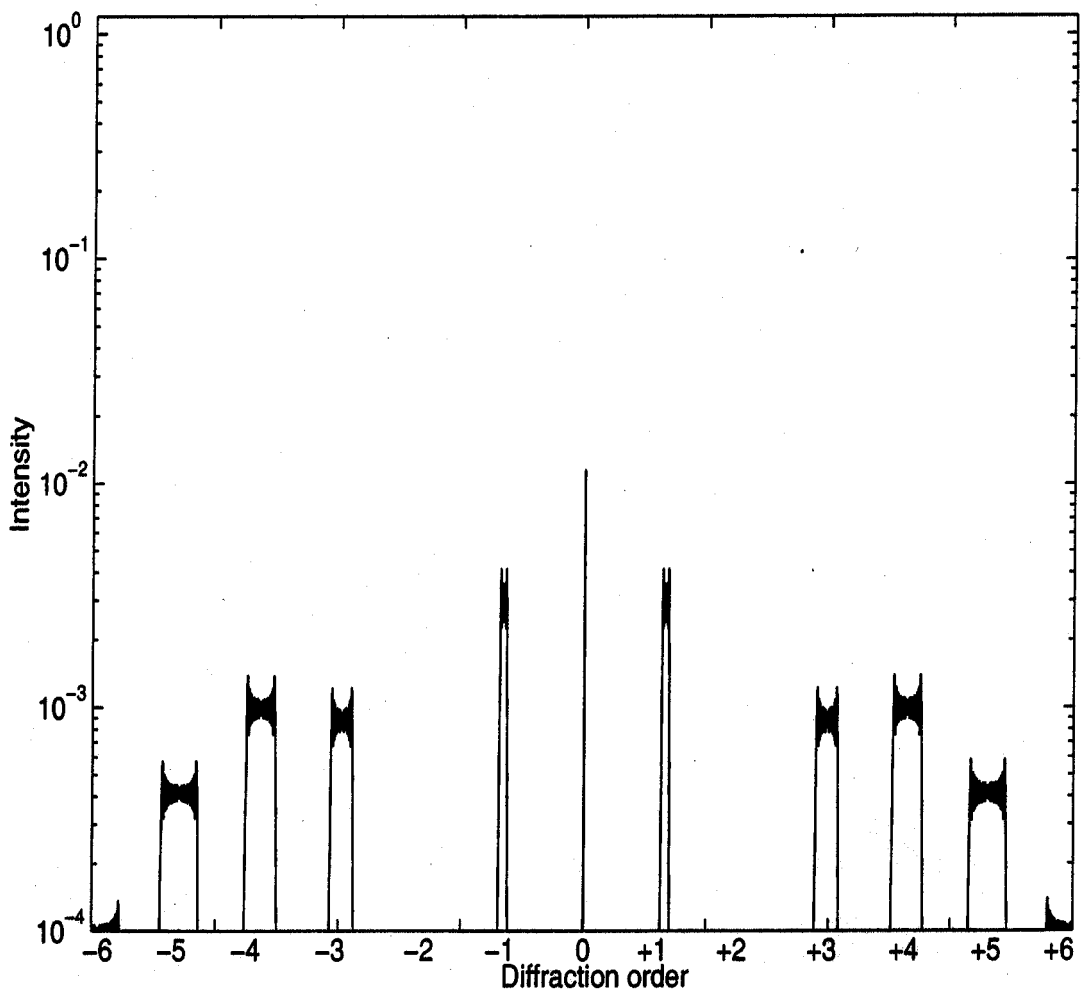

Figure 5.6: Diffraction from a type-I1 sample illuminated with a uniform input beam. Here the pitch at one end of the sample is 20pm and it linearly increases to 22μm at the other end.

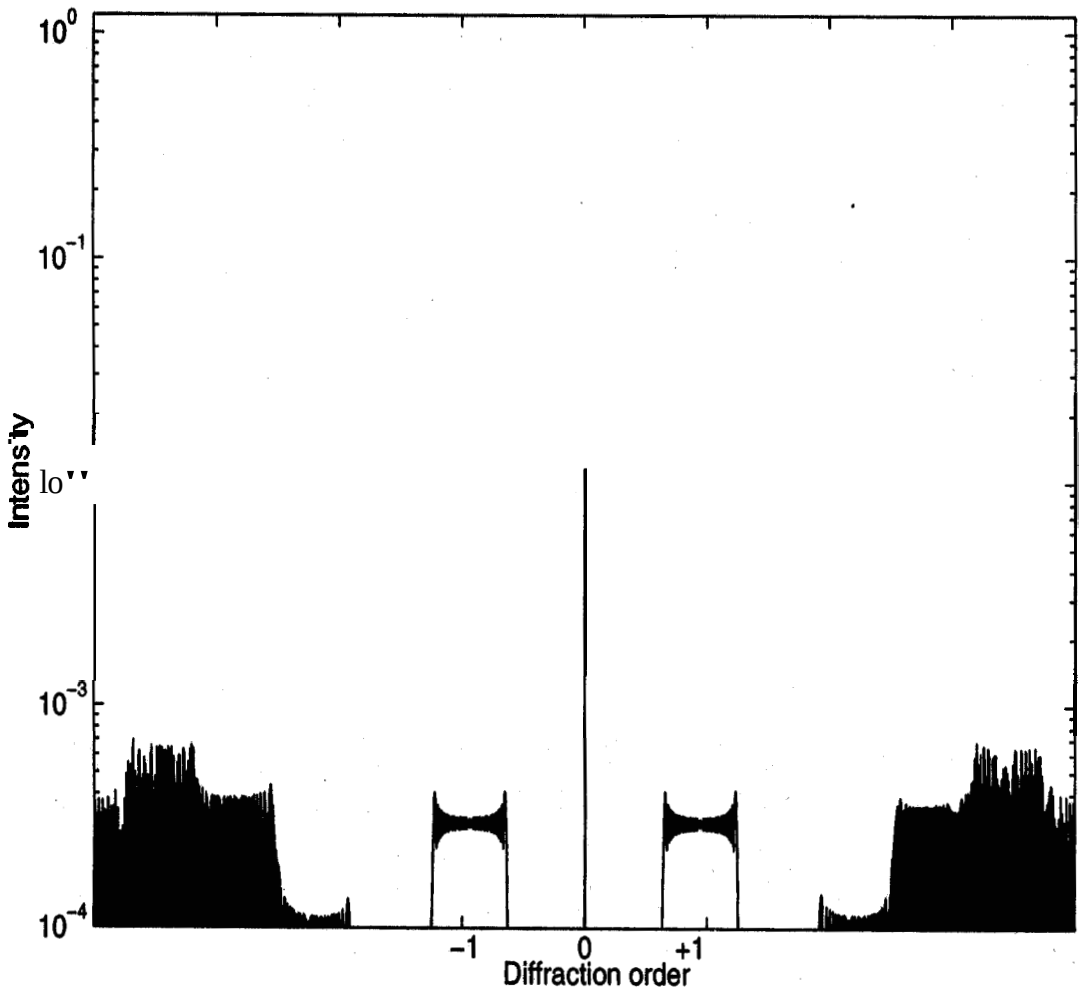

Figure 5.7: Diffraction from a type-I1 sample where the pitch at one end of the sample is 20μm and at the other end is 40μm.

metry becomes more prominent. In figure(5.11) the tapering of the profiles of the orders ±4 and ±5 is very clearly seen. Also, the intensity of each order considerably drops with increase in the pitch gradient.

We now describe the computed diffraction patterns for the type-Ib cholesteric. In figure(5.12) we show the diffraction pattern from such a cholesteric. Here, the cholesteric has a pitch gradient such that the pitch at the center is 5% lower than the pitch at the ends. We observe that the profile of each order is asymmetric with respect to its center. Like in the previous case, here also they have saw-tooth like profiles. But unlike the previous case they taper towards the zeroth order. Here again, there is a broadening of the profiles as we go to higher orders. When the pitch gradient is further increased these features become more and more prominent. The diffraction patterns for the samples with 20% and 50% pitch gradients are shown in figures(5.13) and (5.14) respectively. We note that each order of the diffraction pattern from type-Ia is a mirror image of its counterpart in the diffraction pattern from type-Ib.

We now consider the diffraction patterns from the type-II cholesterics. In figure(5.15) we depict the diffraction pattern from a type-II sample with a pitch gradient such that the pitch at the sample center is 5% higher than the pitch at the lower end. One may notice that the profiles of the orders become broad and smooth. The diffraction pattern from the type-II structure appears as a convolution of a Gaussian profile with the diffraction pattern from a uniform cholesteric. As the pitch gradient is increased, the profiles of the higher orders become broader and their peak intensities decrease. The diffraction pattern for a type-II cholesteric where the pitch at the sample center is 20% and 50% higher than the pitch at the lower end are shown in figures(5.16) and (5.17) respectively.

In the experiments, it may not be possible to exactly match the centre of the Gaussian beam and the centre of the cholesterics of the type-Ia or the type-Ib. Hence, we have also performed computations to check the effect of a shift between the center of the Gaussian beam and the center of the structure of the type-Ia or the type-Ib

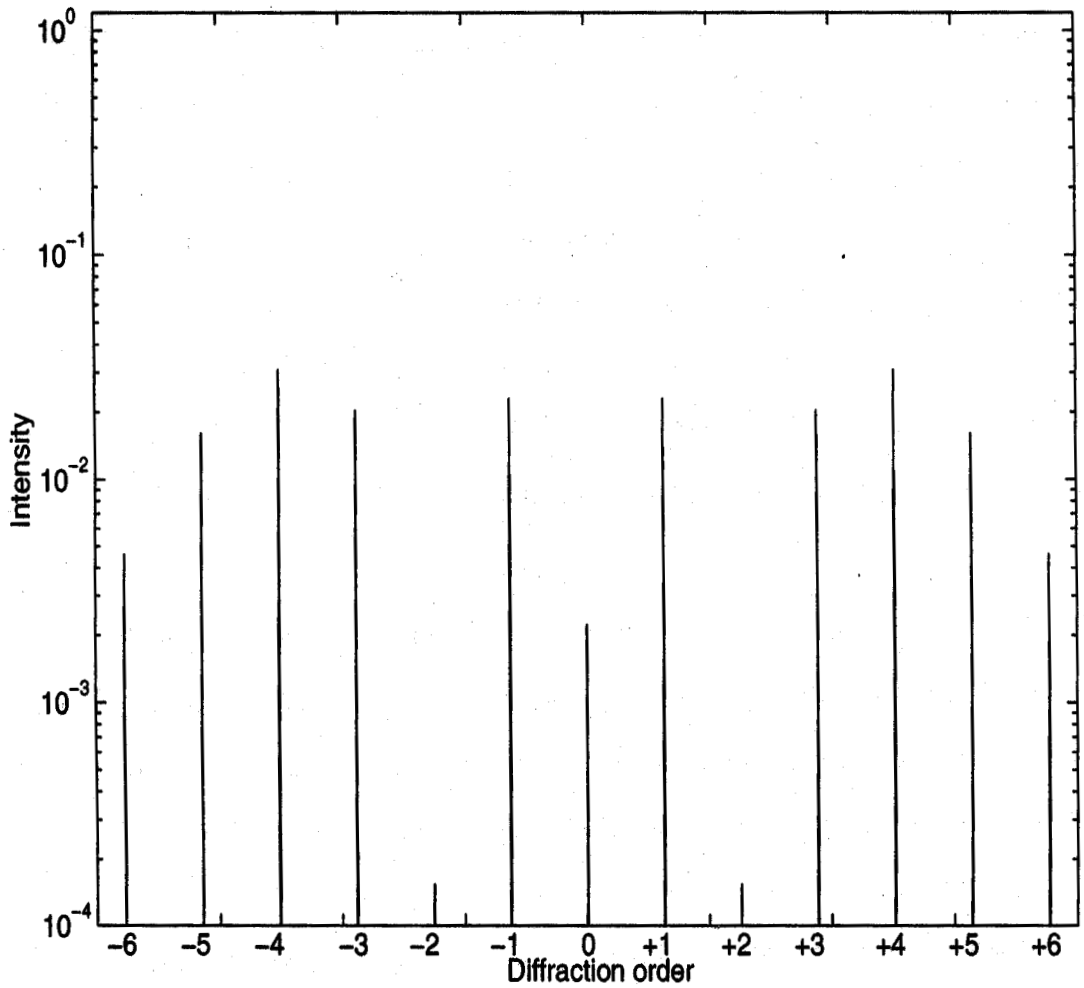

Figure **5.8:** Diffraction pattern of a uniform cholesteric with a Gaussian input beam. Here, the cholesteric structure has a pitch of 20μm. Here, the lateral sample size is 100x20 μm=2mm. The input beam has a Gaussian intensity width of $\sigma/\sqrt{2}$, where σ=1mm.

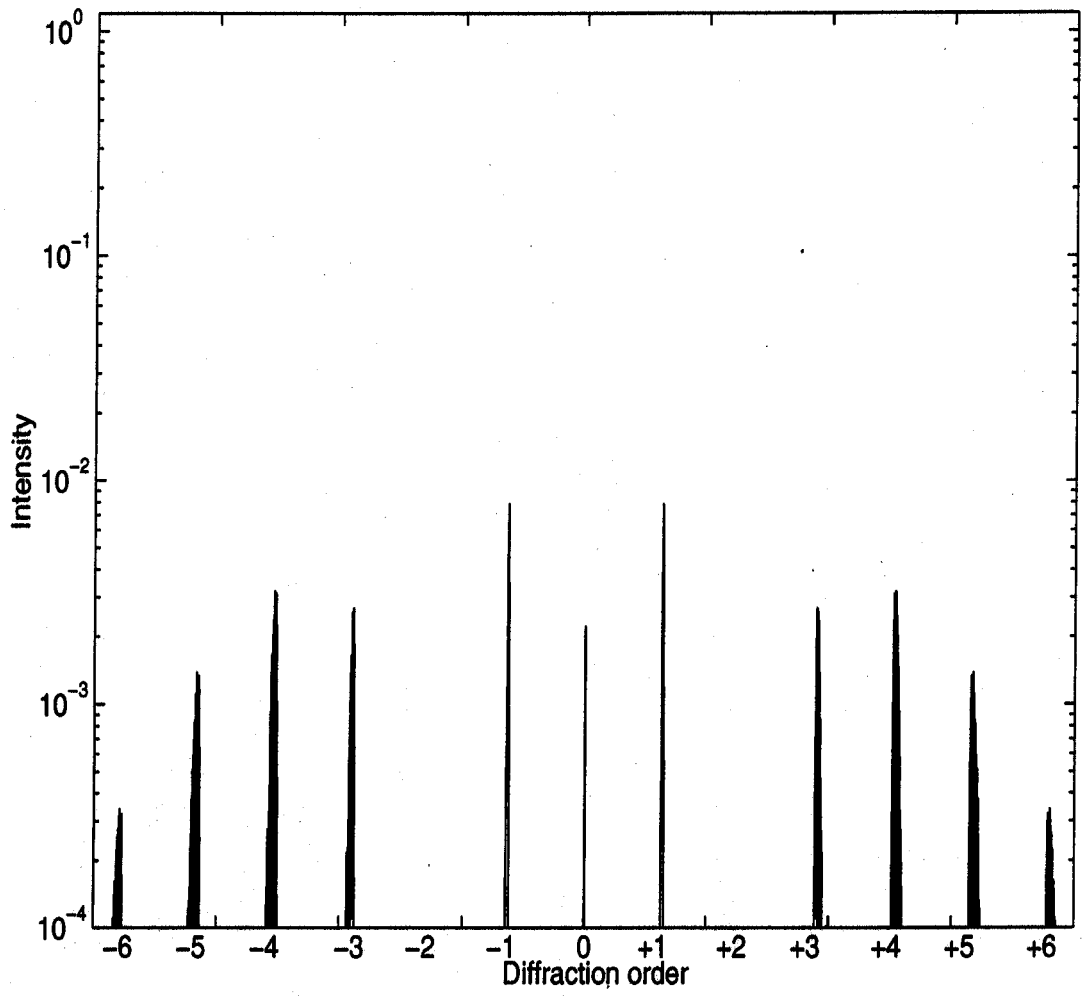

Figure 5.9: Diffraction from a type-Ia sample with a Gaussian input beam. The pitch at the center is 21μm and at the ends is 20μm. Here, the Gaussian intensity width is the same as that given in figure(5.8).

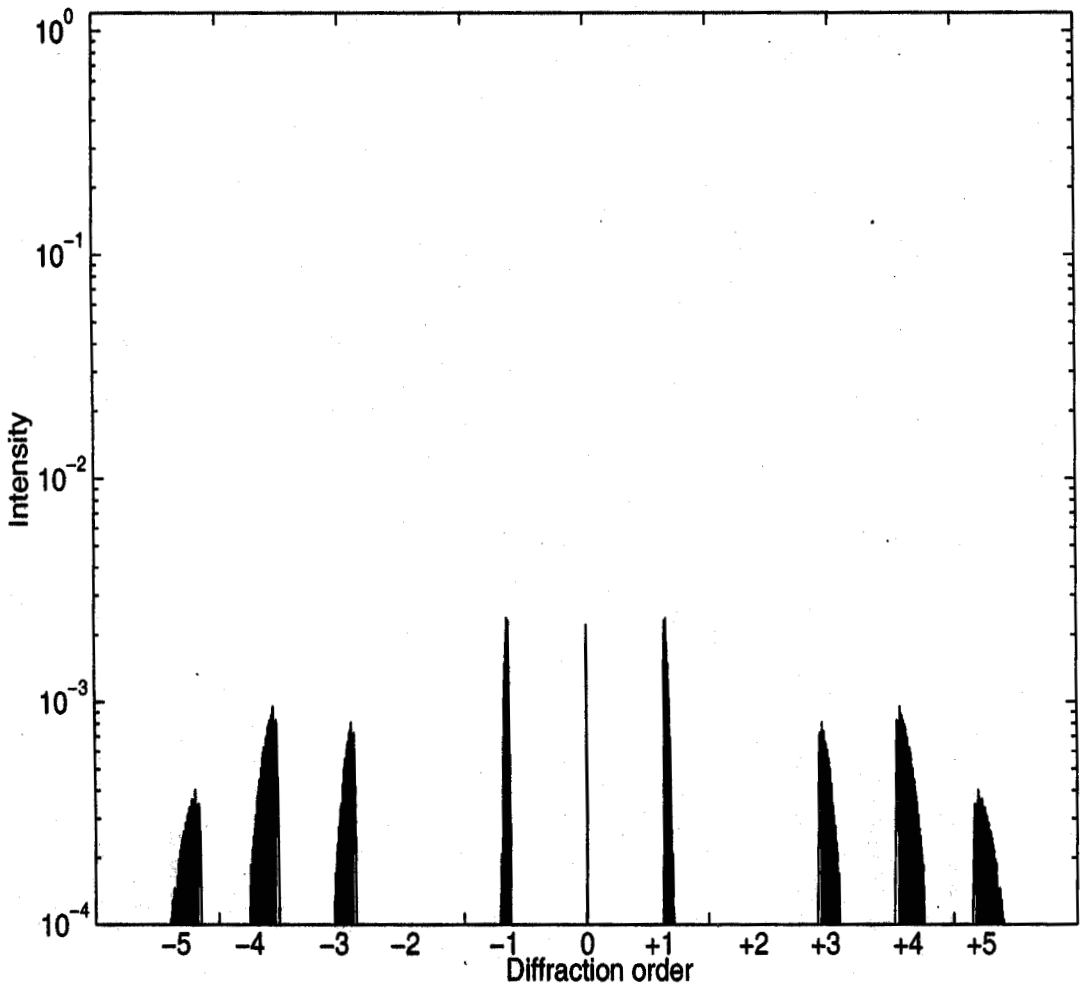

Figure 5.10: Diffraction from a type-Ia sample with a Gaussian input beam. The pitch at the center is 24μm and at the ends is 20μm. Here, the Gaussian intensity width is the same as that given in figure(5.8).

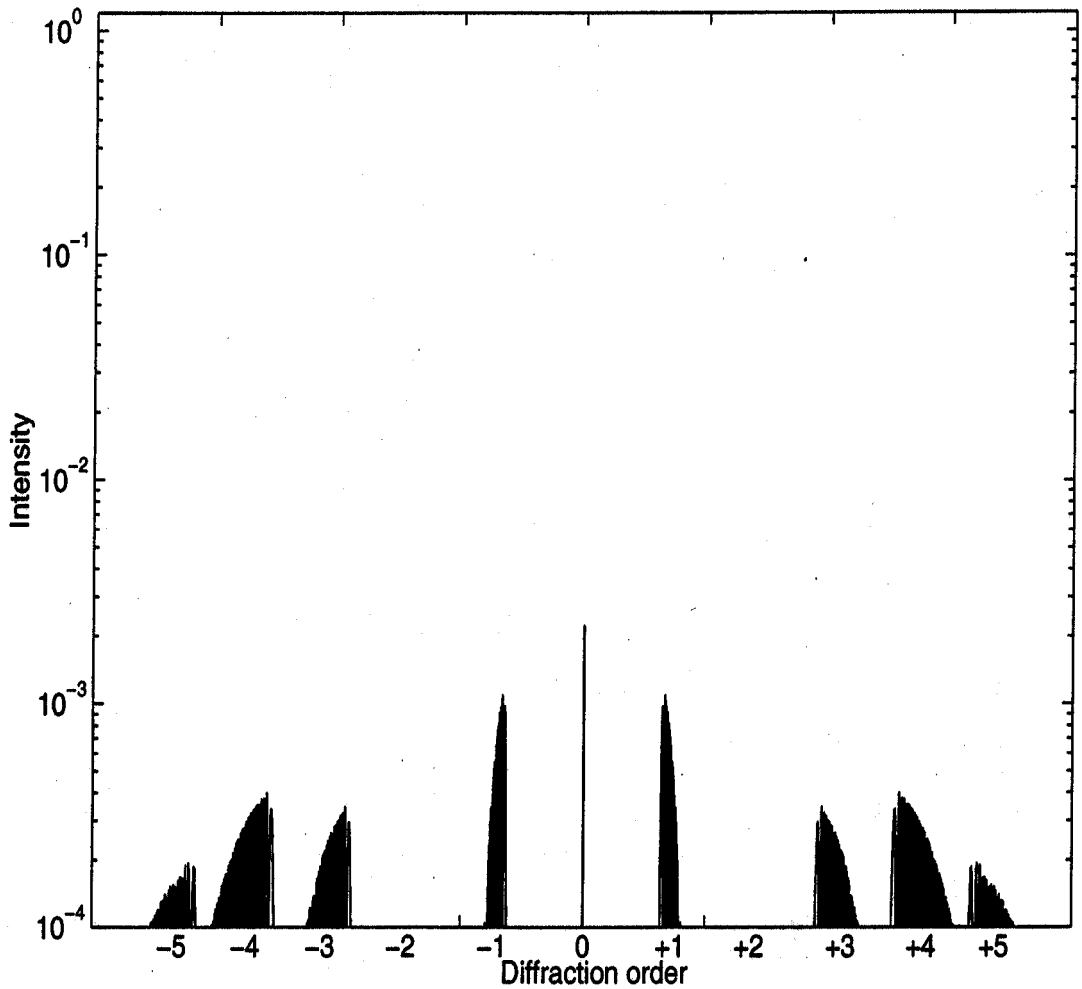

Figure 5.11: Diffraction from a type-Ia sample with a Gaussian input beam. The pitch at the center is 30μm and at the ends is 20μm. Here, the Gaussian intensity width is the same as that given in figure(5.8).

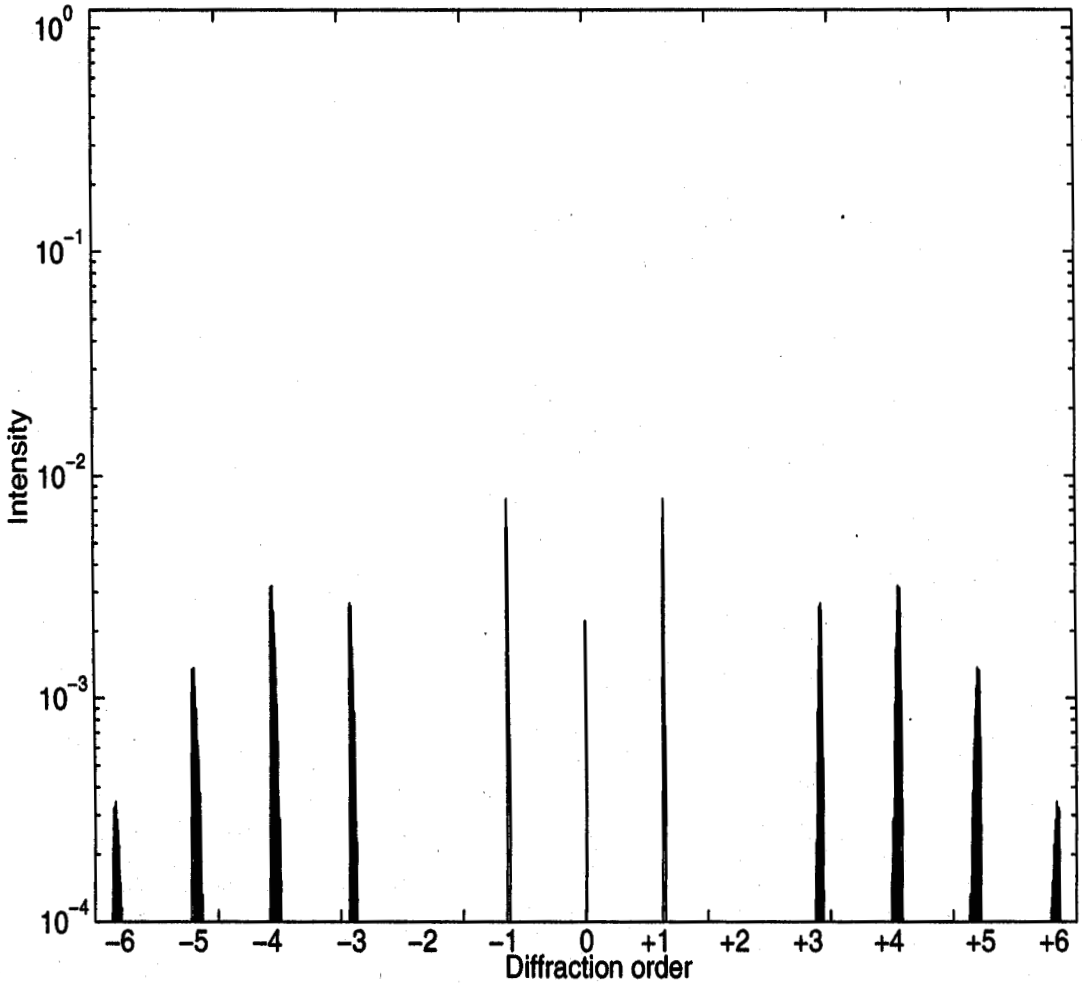

Figure 5.12: Diffraction from a type-Ib sample with a Gaussian input beam. The pitch at the center is $19\mu m$ and at the ends is $20\mu m$. Here, the Gaussian intensity width is the same as that given in figure(5.8).

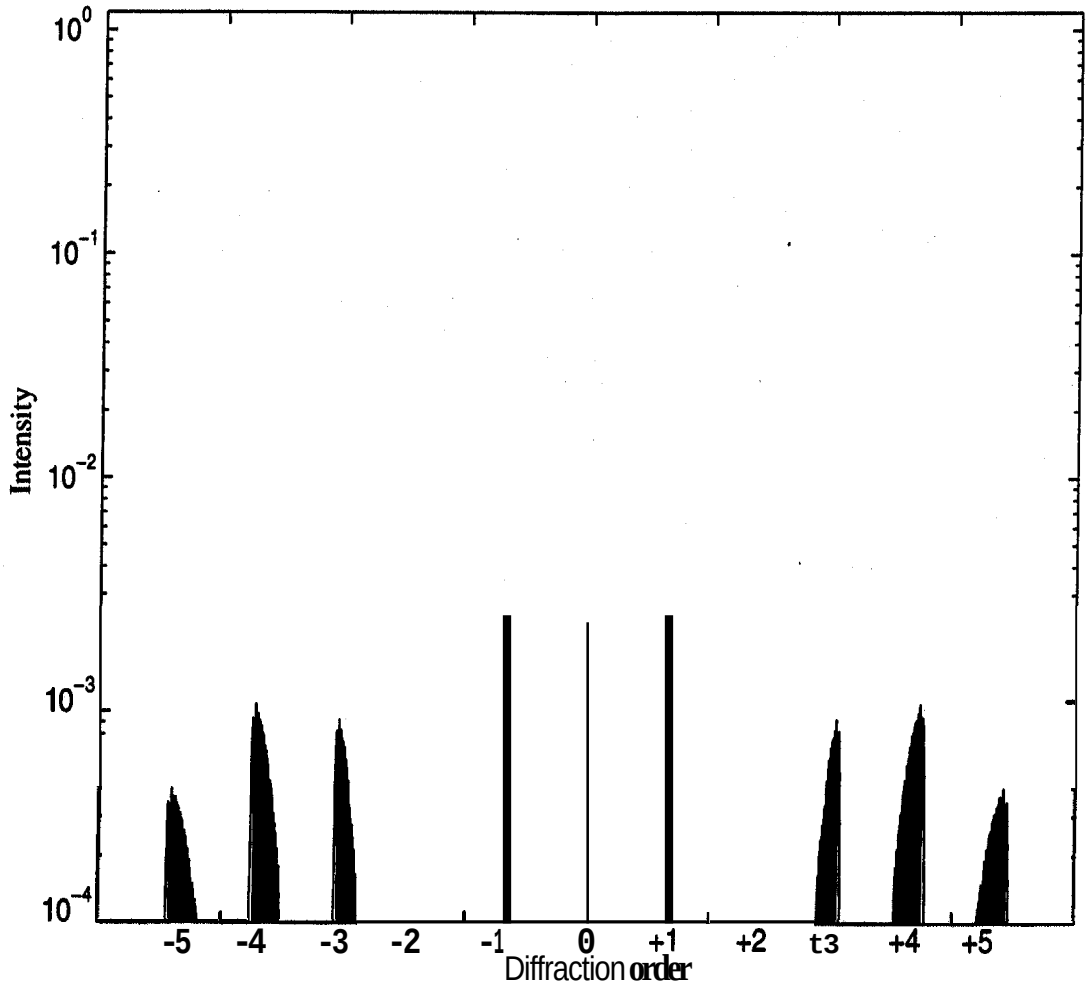

Figure 5.13: Diffraction from a type-Ib sample with a Gaussian input beam. The pitch at the center is $16\mu m$ and at the end is $20\mu m$. Here, the Gaussian intensity width is the same as that given in figure(5.8).

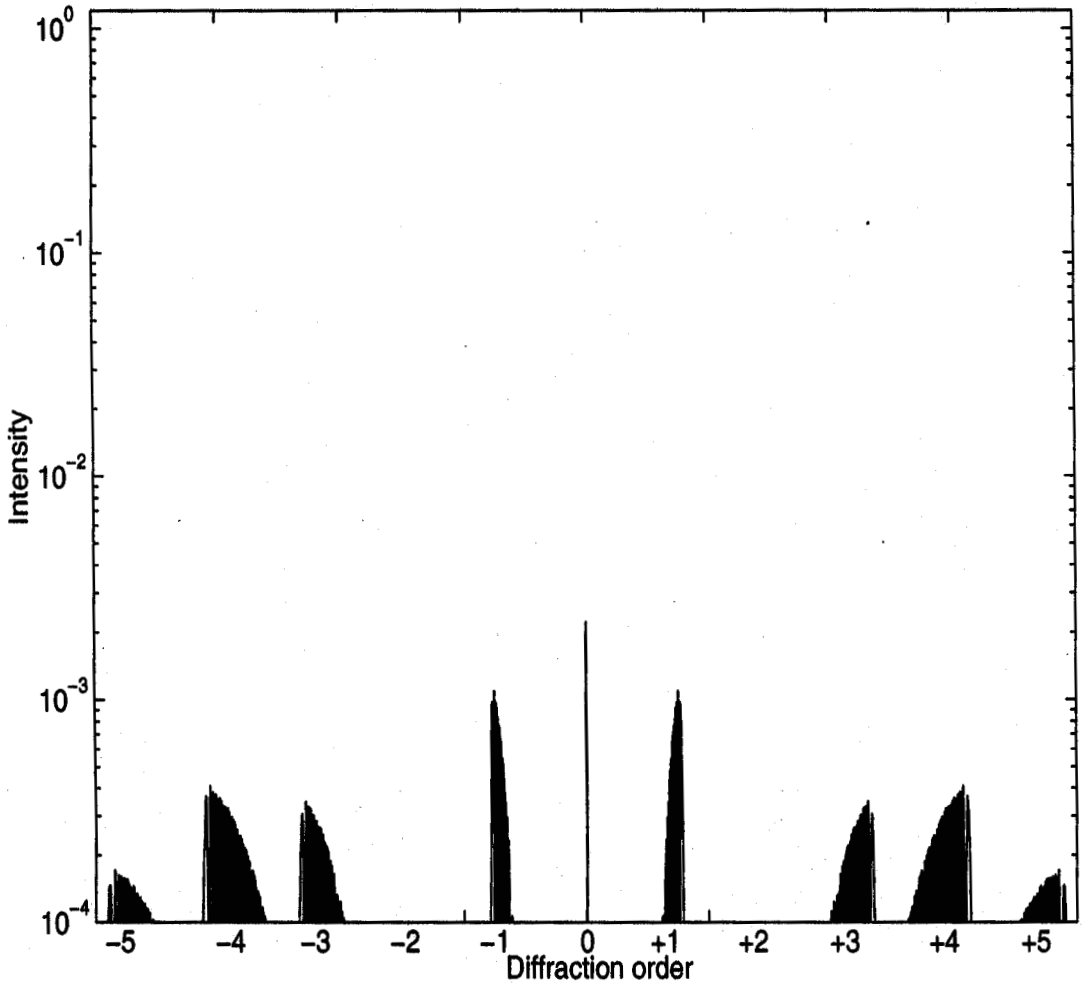

Figure 5.14: Diffraction from a type-Ib sample with a Gaussian input beam. The pitch at the center is $10\mu m$ and at the end is $20\mu m$. Here, the Gaussian intensity width is the same as that given in figure(5.8).

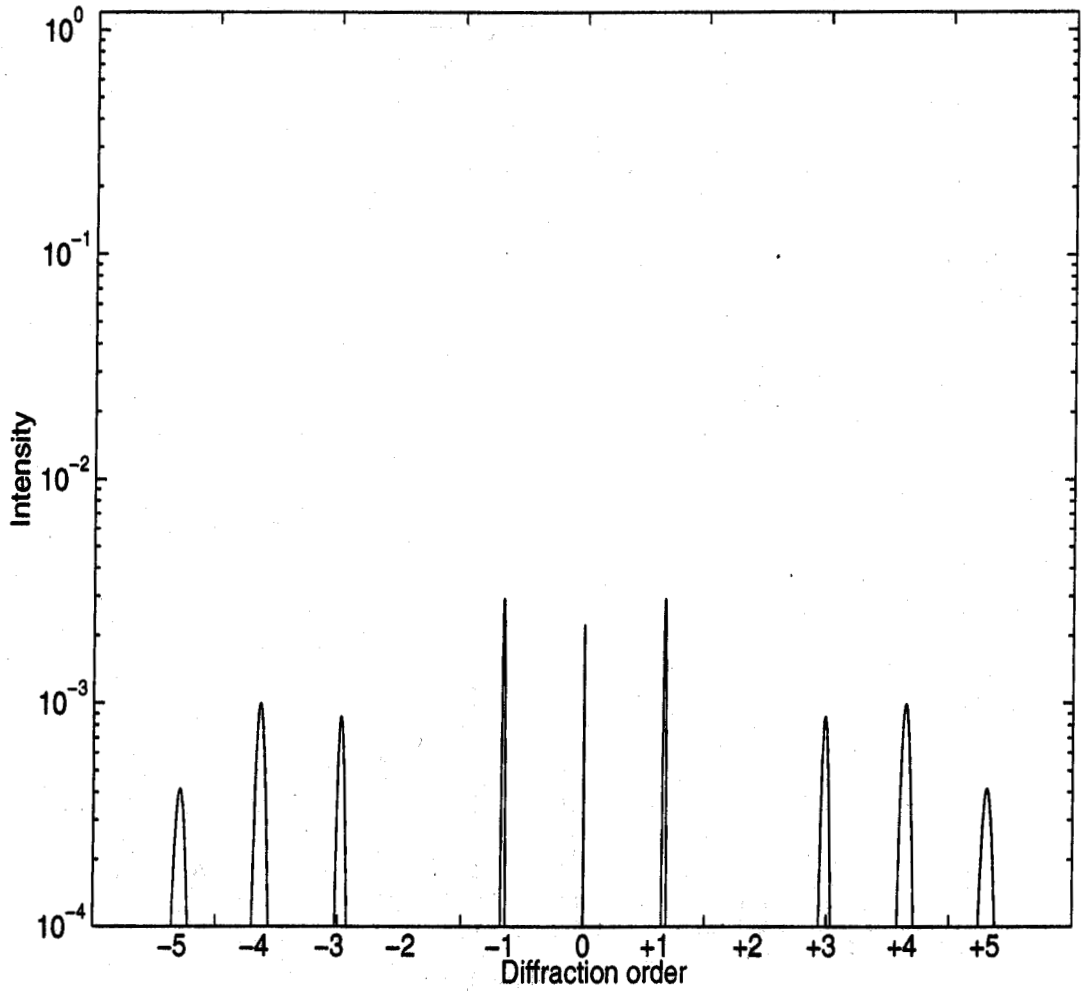

Figure 5.15: Diffraction from a type-I1 sample with a Gaussian input beam. The pitch at one end of the sample is 22μm and linearly reduces to 20μm at the other end of the sample. Here, the Gaussian intensity width is the same as that given in figure(5.8).

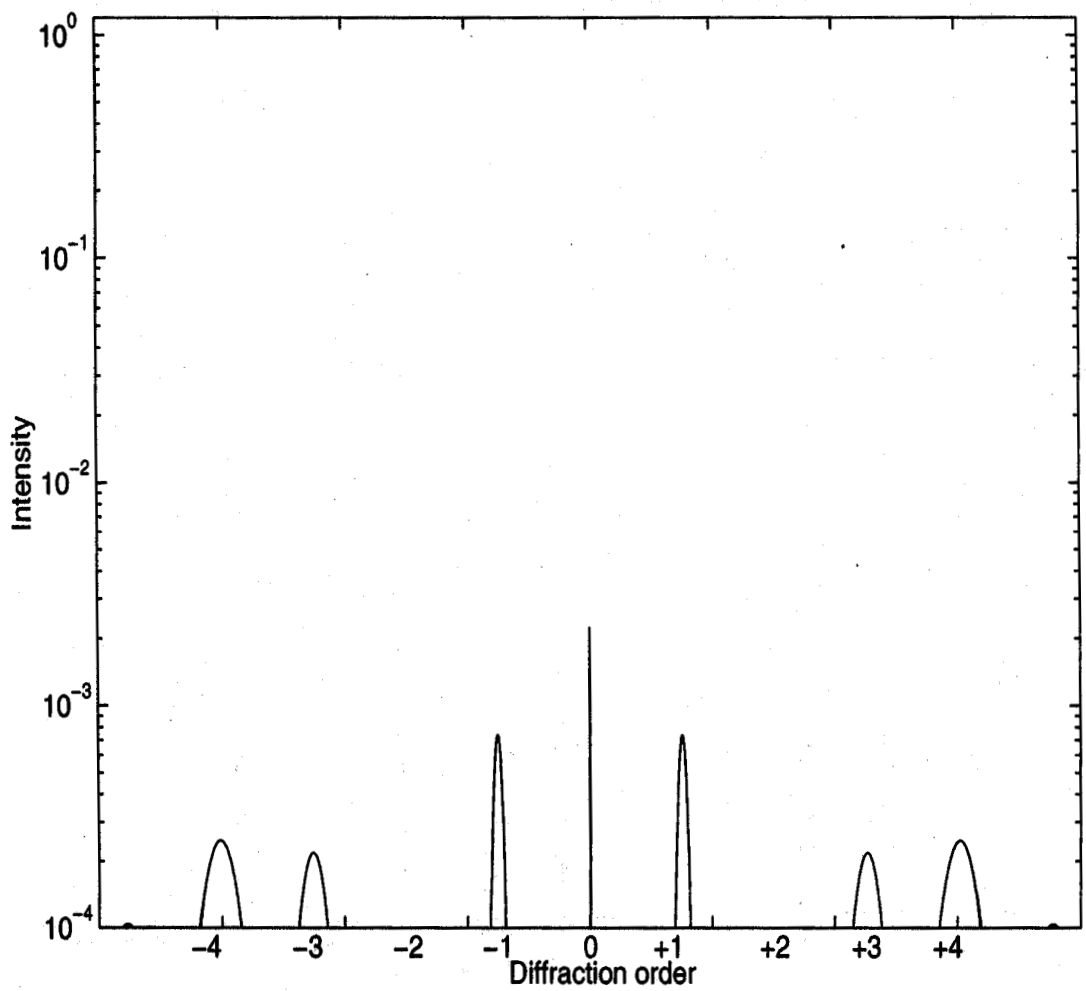

Figure 5.16: Diffraction from a type-I1 sample with a Gaussian input beam. The pitch at one end of the sample is 28μm and linearly reduces to 20μm at the other end of the sample. Here, the Gaussian intensity width is the same as that given in figure(5.8).

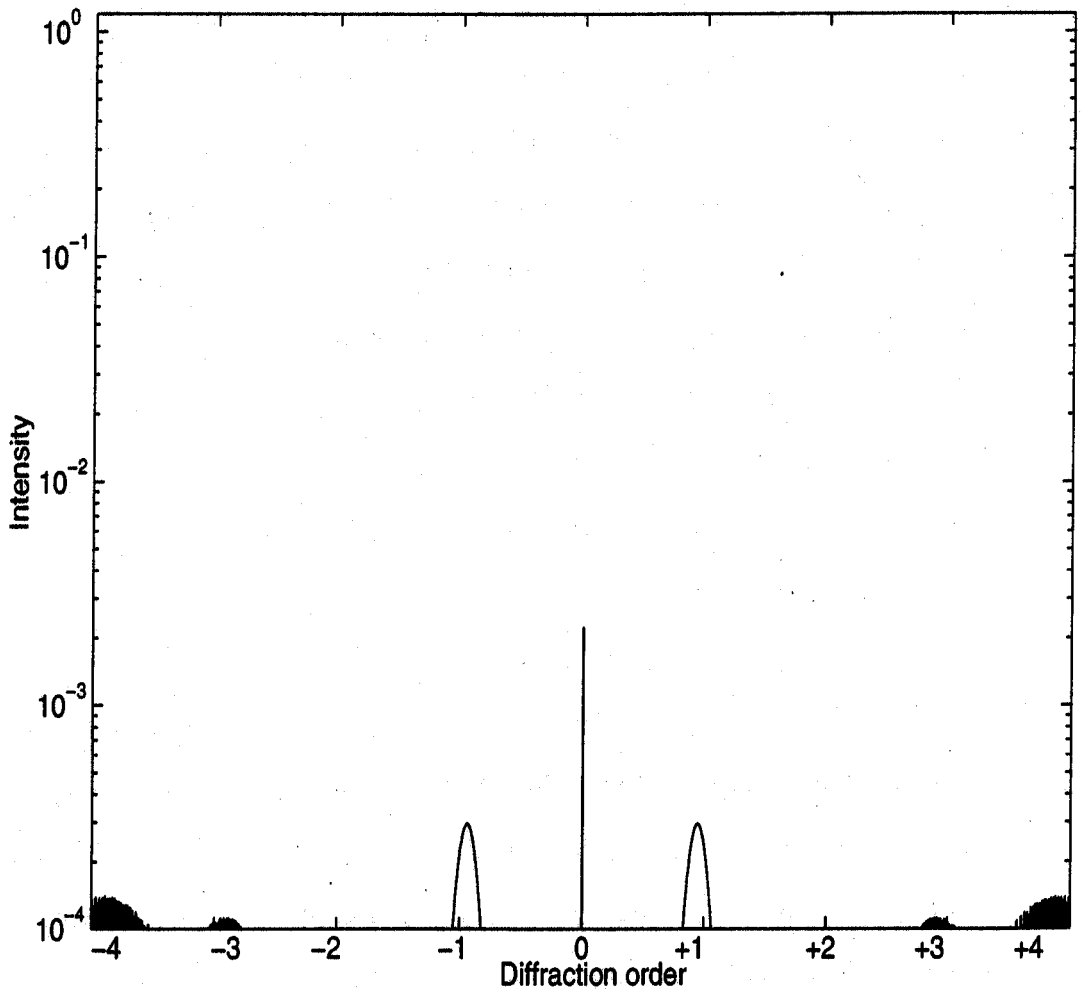

Figure 5.17: Diffraction from a type-II sample with a Gaussian input beam. The pitch at one end of the sample is 40pm and linearly reduces to 20pm at the other end of the sample. Here, the Gaussian intensity width is the same as that given in figure(5.8).

cholesterics. We find that shifts up to 10% of the Gaussian width do not alter the diffraction profiles considerably.

5.4 Discussion

In practice, cholesteric samples are always of non-uniform pitch to some extent. For certain applications, the non-uniformities in the cholesterics can be carefully engineered to obtain specific optical properties [4]. Our computations of the diffraction pattern in the phase grating geometry with uniform and Gaussian input beams yield some very interesting results. We find that the diffraction orders are very sensitive to pitch gradients as small as even 5% of the uniform pitch. We have considered two types of non-uniformities, one, with the pitch gradient symmetric with respect to the center of the sample and the other, with the pitch gradient asymmetric with respect to the center of the sample. In both cases, we find that the peak intensities of the diffraction orders drop significantly accompanied with a marked increase in the widths of the diffraction orders.

With uniform input beams, the diffraction patterns for the type-Ia and the type-Ib structures are nearly indistinguishable. On the other hand, with Gaussian input beams, the patterns for type-Ia and type-Ib structures are very different. Here, each diffraction order exhibits a tapering saw-tooth profile and the directions of tapering are opposite in the two cases. This difference in the profile shapes is a clear indication of the type of structural asymmetry in the cholesteric.

In practice, laser beams have Gaussian intensity profiles. The widths of these profiles with respect to the lateral sample size, L, is important to observe the characteristics of the diffraction profiles. In our calculations we have taken the value of the Gaussian amplitude width σ to be equal to 1mm. Therefore the width $\sigma/\sqrt{2}$ of the Gaussian intensity profile is much smaller than the lateral sample size of nearly 2mm (given by the product of the average pitch and the number of pitches). Our computations show

that when a is increased, as is to be expected, the diffraction pattern approaches that of a uniform input beam.

The diffraction patterns from the type-I1 cholesterics will have an overall asymmetry about the zeroth order, because this is always true of phase gratings which are asymmetric about their centers. This asymmetry is too small to be seen at the intensity level 10^{-4}. It is worth mentioning here that our results do not show the presence of satellites found in amplitude gratings with gradients in the lattice parameter [9].

It is well known, from the theory of diffraction that broadening of diffraction spots can also occur due to the finite size of the diffraction grating. In an ideal situation, the incident plane wavefront and the lateral sample size L should be infinite. In such a case, the Fourier transform of the corrugated wavefront has to be carried out from $-\infty$ to $+\infty$. Such a condition is difficult to impose in a numerical technique, where one considers finite array sizes, or in experiments where one has a finite lateral sample size. This gives rise to the broadening of the diffraction orders even in the absence of non-uniformities. We have computed the diffraction patterns for different lateral sample sizes for uniform input beams using equation(5.8). This is shown in figure(5.18). We find that the effect is pronounced only when the sample size or equivalently number of pitches is of the order of 20. Our computations are carried out for 100 pitches where the finite size effects on diffraction broadening are found to be negligible.

There is one another process that can again lead to broadening of a diffraction order. This process is well established in crystals. X-ray diffraction from crystals with thermal fluctuations of the lattice give rise to a diffuse background and the broadening of the sharp diffraction spots. To find this contribution in cholesterics, we have investigated the thermal effects, on the diffraction orders. We have considered for simplicity only the in-plane thermal fluctuations of the director which in turn lead to fluctuations in the pitch.

The distortion free energy density of a planar cholesteric for pitch changes is given

by,

$$F_d = \frac{K_2}{2}\left(\frac{\partial \theta_z}{\partial z} - q_o\right)^2 \tag{5.10}$$

where θ_z is the director orientation at z and K_2 is the twist elastic constant. In an ideal cholesteric $\theta_z = q_o z$. Let a dimensionless quantity u(z) represent the instantaneous spatial non-uniformity in orientation caused by the random thermal fluctuations [10]. The director configuration is then modified to,

$$\theta' = q_o z + u(z) \tag{5.11}$$

u(z) can be decomposed into its individual Fourier components

$$u(z) = \sum_{q=q_{min}}^{q_{max}} u_q e^{iqz} \tag{5.12}$$

where the cut-off wave vectors are given by

$$q_{min} = \frac{2\pi}{L} \tag{5.13}$$

$$q_{max} = \frac{2\pi}{p} \tag{5.14}$$

where p is of molecular dimensions.

Equations(5.10), (5.11) and (5.12) lead to the energy of a mode of wavevector **q.** According to the equipartition theorem, the energy of each mode is,

$$\frac{1}{2}k_B T$$

Here k_B is the Boltzmann constant and T is the absolute temperature.

This leads to the average amplitude square of a thermal fluctuation of wavevector q [10]. It is given by,

$$\langle |u_q|^2 \rangle = \frac{k_B T}{q^2 K_2} \tag{5.15}$$

Using this model for the thermal fluctuations with typical values of K_2 we have calculated the diffraction pattern at a temperature of 300 K. We find very little detectable change in the widths of the diffraction orders due to the thermal fluctuations. Our

results indicate that the thermal fluctuations of the pitch of a cholesteric have no appreciable effects on the widths of the diffraction orders.

These results indicate that the usually observed broadening of the diffraction orders in cholesterics are mainly due to the gradients in the pitch arising due to the local strains rather than the thermal fluctuations of the pitch or the sample size effects.

Cholesteric phase gratings find applications in signal processing where the intensity, direction and other features of the diffraction orders are exploited [11]. Our results show that the gradient in the pitch drastically changes the intensity and profile of the orders and thus adds a new dimension to tuning the signal. The gradient in the pitch of the cholesteric can be easily manipulated by the application of weak electric fields, temperature gradients, mechanical stresses or even by chemical means. Such external stimuli can modulate the features of the diffraction orders in a controlled fashion. This additional property can be exploited to add more tunability in signal processing.

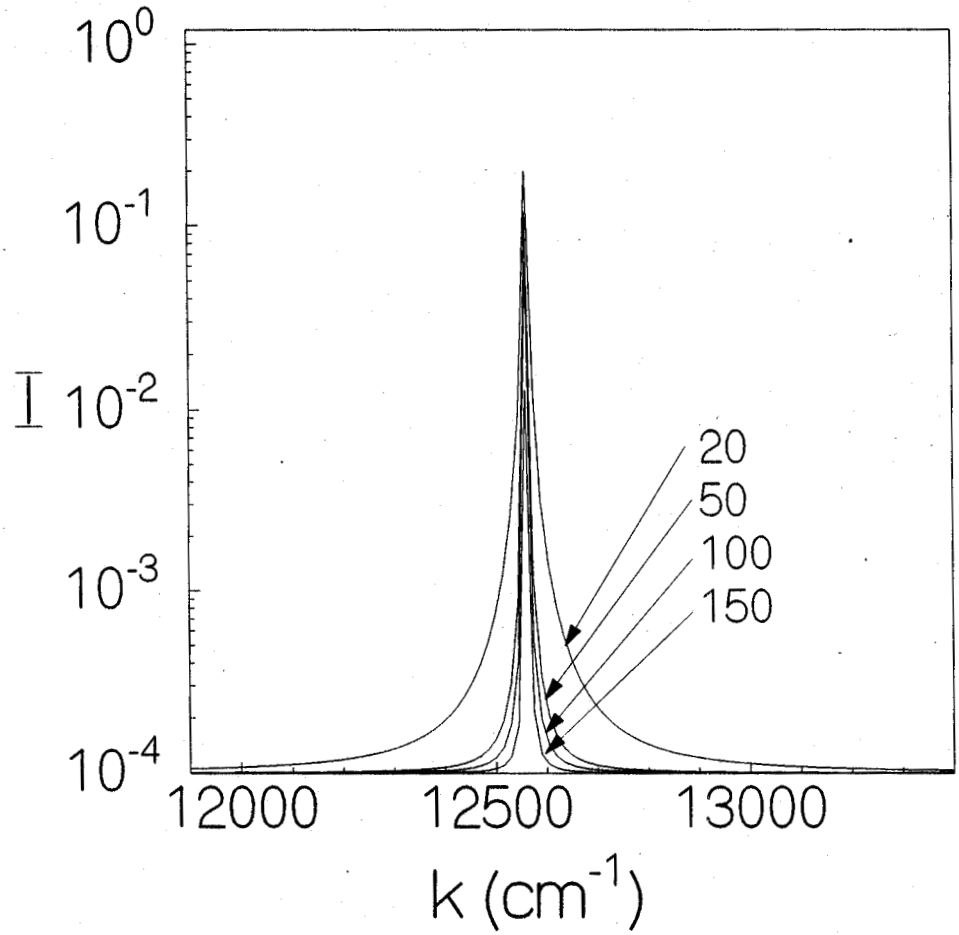

Figure **5.18:** Illustrating the finite size effects on the width of the fourth order diffraction from a uniform cholesteric of pitch **20** μm. Diffraction intensities of the fourth order for samples with **20, 50, 100** and **150** pitches are shown. It can be seen that the difference in the widths of the profiles between the **20** and **50** pitch samples is much more than the difference between the widths of the profiles calculated for the **100** and **150** pitch samples. For smaller sample size, there is a decrease in the peak intensity but it is too small to be seen in the figure.

Bibliography

[1] S. Chandrasekhar. Liquid Crystals , 2nd. ed., Cambridge University press, Cambridge (1992).

[2] S. Mazkedian, S. Melone, and F. Rustichelli. J. Phys. (Paris), Supplement C1, 283 (1975).

[3] R. Bartolino and N. Scaramuzza. Symmetries and broken symmetries in condensed matter physics. page 385, IDSET-Paris, (1981). Proceedings of the Colloque Pierre Curie.

[4] D. J. Broer, J. Lub, and G. N. Mol. Nature, 378, 467 (1995).

[5] C. V. Raman and N. S. Nagendra Nath. Proc. Ind. Acad. Sci., A, 2, 406 (1935).

[6] K. A. Suresh, P. B. Sunil Kumar, and G. S. Ranganath. Liquid Crystals, 11, 73 (1992).

[7] E. Sackmann, S.Meiboom, L. C. Sydner, A. E. Meixner, and R. E. Dietz. J. Am. Chem. *Soc.*, 90, 3567 (1968).

[8] J. G. Proakis and D. G. Manolakis. Digital Signal Processing, Principles, Algorithms and Applications. Prentice Hall of India, New Delhi (1995).

[9] H. Lipson S. G. Lipson and D. S. Tannhauser. Optical Physics. Cambridge University Press, Cambridge (1995).

[10] P. G. de Gennes and J. Prost. The Physics of Liquid Crystals (2nd ed.). Clarendon press, Oxford (1993).

[11] **D. Subacius, S. V. Shiyanovskii, Ph. Bos, and O. D. Lavrentovich. Appl.** *Phys. Lett.*, **71, 3323 (1997).**